第 43 卷 第 21 期/2023 年 11 月/光学学报 研究论文

光学学报

双金属锥形光纤表面增强拉曼散射探针拉曼增强特性

黄博，汪正坤，朱永*，张洁

重庆大学光电技术及系统教育部重点实验室，重庆 400044

摘要 为了提高金属纳米粒子在光纤表面的富集密度，同时提高光纤表面增强拉曼散射（SERS）复合结构拉曼增强特性的稳定性，提出一种双金属（金和银）锥形光纤SERS探针结构。首先，采用化学还原法制备出形貌均一的金银纳米粒子；然后，采用光诱导的方法实现双金属在锥形光纤上的富集。制备的光纤SERS探针表现出良好的实验效果：对罗丹明6G（R6G）检测到的最低浓度低至10^{-10} mol/L；增强因子为2.07×10^{8}；相较于单金属银光纤SERS探针，双金属样品的稳定性提高了7倍（96 h后）。

关键词 散射；拉曼散射；双金属；锥形光纤；光诱导

中图分类号 TN252 **文献标志码** A **DOI**：10.3788/AOS230953

1 引 言

表面增强拉曼散射（SERS）是一种强大的分析工具，能够提供分子的振动“指纹”信息。由于其独特的分析优势，SERS在生物医学[1-2]、环境保护[3-4]、食品检测[5-6]等领域得到了广泛的应用。

1974年，Fleischmann等[7]发现当有机分子吡啶被吸附在粗糙的金属表面时，拉曼信号会被显著增强。此后，科学家们开始研究如何用各种贵金属纳米粒子基底放大拉曼信号。虽然银纳米粒子由于其出色的局域表面等离子体共振特性常被用作SERS基底，但其易被氧化的缺点使得在构建纳米探针的应用中受到很大限制。相比之下，金纳米粒子的化学稳定性更好、生物毒性更低，但拉曼信号增强能力相对较弱[8]。因此，很多科学家将研究重点放在了双金属基底方面。例如：Bian等[9]通过一步法制备了SiO_2@Au/Ag合金核壳纳米粒子并实现了对结晶紫（CV）拉曼信号的有效放大；Shinki等[10]利用共聚焦磁控溅射系统共溅射Au和Ag，在锥体硅表面沉积Au和Ag比例为1∶1的合金薄膜，实现了对浓度为10^{-9} mol/L的罗丹明6G（R6G）的检测；Li等[11]通过化学合成法制备了Au-Ag核壳纳米金字塔，用于生物相关小分子的SERS鉴别。为了进一步将SERS技术应用于原位监测和远程检测方面[12]，光纤是一种很好的选择。

光纤作为信号远程传输的良好载体，将其与SERS结合起来，可以在远程检测方面提供更便利的条件。此外，锥形光纤不仅可以将倏逝场传递到周围环境中，而且增加了倏逝场作用范围。因此，它具有增强激光反射和提高集光能力的巨大潜力，这对于收集弱拉曼信号、获得更低的检测极限非常有帮助[13]。基于这些优点，大量的锥形光纤SERS探针被制备出。例如：Yu等[14]在锥形光纤上富集了银纳米粒子，并结合腔增强技术成功地检测到浓度为10^{-11} mol/L的R6G；Liu等[15]制备了环状锥形光纤SERS探针，对CV的检测极限为2×10^{-10} mol/L；Cao等[16]利用硅烷化处理后的锥形光纤合成了光纤SERS探针，成功检测到4-氨基苯硫酚（4-ATP），检测极限为10^{-9} mol/L。尽管上述锥形光纤实现了低检测极限和信号远程传输，但均在光纤尖端上沉积单金属纳米粒子来增强拉曼信号，忽略了双金属的卓越光学性能。因此，有必要制备一种双金属锥形光纤SERS探针，以获得更低的检测极限和更高的稳定性。

针对上述问题，本文提出一种简单经济的双金属锥形光纤SERS探针，该探针利用自组装的方式在锥形光纤表面上沉积金银纳米粒子，具有高灵敏度和良好的稳定性。

2 实验部分

2.1 锥形光纤制备

利用拉锥机（FSCW-3000，中国山东福寿光电子

收稿日期：2023-05-09；**修回日期**：2023-06-01；**录用日期**：2023-06-16；**网络首发日期**：2023-06-26

基金项目：国家自然科学基金（62175023）、重庆市杰出青年基金（cstc2019jcyjjqX0018）

通信作者：*yongzhu@cqu.edu.cn

通信有限公司生产)制备锥形光纤,如图 1(a)所示,主要步骤如下:首先,取 90 cm 纤芯/包层为 62.5/125 μm 的多模光纤,去除中间部分约 2 cm 长的涂覆层,用酒精擦拭裸露部分保持清洁;接着,将其夹持在光纤夹具上,并确保裸露部分位于火头的正下方;然后,将导轨运行距离设置为 1.8 cm,运行速度设置为 0.5 cm/min,并开启拉锥机开始拉制;当拉制完成后(此时,光纤将会从中间位置处拉断)即可得到两根锥形光纤。

2.2　金属纳米粒子制备

采用一步还原法制备银纳米粒子[17],其中,氢氧化钠和氯化银均为 2.5 mL,在黑暗条件下持续搅拌 2 h,即可得到粒径约为 50 nm 的银纳米粒子。采用氯金酸还原法制备金纳米粒子[18],具体步骤如下:首先,配置质量分数为 1% 的氯金酸溶液;其次,配置质量分数为 1% 的柠檬酸钠溶液;然后,将 1 mL 质量分数 1% 的氯金酸溶液加入 99 mL 去离子水中,再向其中加入 1 mL 1% 的柠檬酸钠溶液;接着,将溶液加热至沸腾并保持 15 min;最后,自然冷却即可得到平均粒径为 50 nm 的金纳米粒子。

2.3　锥形光纤 SERS 探针制备

采用光诱导的方法将金纳米粒子(AuNPs)和银纳米粒子(AgNPs)富集在锥形光纤尖端,具体的实验流程如图 1 所示。首先,将氦氖激光器(HJ-1B)发出的激光耦合进锥形光纤(波长为 632.8 nm,激光出射功率约为 1 mW);接着,将锥形端浸入 Ag 溶胶和 Au 溶胶(体积比为 1∶1,两者均为 0.3 mL)的混合溶胶,持续 60 s;随后,将锥形端从溶液移至空气中持续 90 s,保持激光器工作。重复以上步骤 15 次,待整个过程结束后,即可得到如图 1(b)所示的锥形光纤 SERS 探针。

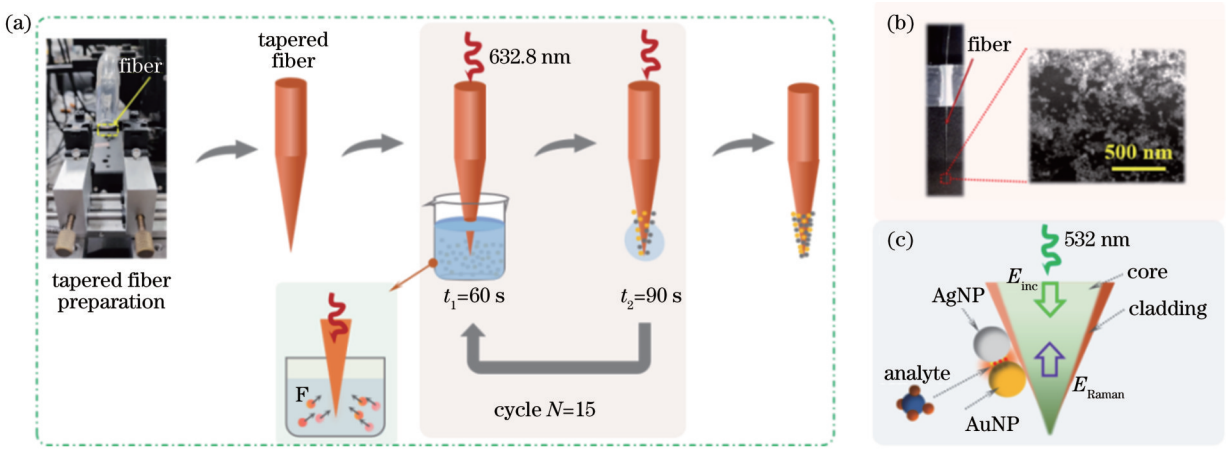

图 1　实验流程图。(a)光纤 SERS 探针制备流程示意图;(b)光纤 SERS 探针实物图及电镜图;(c)拉曼检测示意图

Fig. 1　Experimental flowchart. (a) Schematic diagram of the preparation process of the fiber SERS probe; (b) real image and SEM image of the fiber SERS probe; (c) schematic diagram of Raman detection

2.4　拉曼测试

选择 R6G 作为分析物分子,以检测制备样品的 SERS 性能。将锥形光纤 SERS 探针分别浸入浓度为 10^{-8}~10^{-10} mol/L R6G 溶液中 3 min,然后从溶液中取出,自然干燥后进行拉曼信号的检测。进行多分子检测时,将样品浸入浓度为 10^{-6} mol/L R6G 和 10^{-4} mol/L CV 的混合溶液中 3 min,然后从溶液中取出,自然晾干后进行检测。检测原理如图 1(c)所示,激光通过物镜聚焦在锥形光纤芯上,并传输到光纤的尖端。从末端直接输出的光场和沉积在末端的双金属纳米粒子发生相互作用,极大地增强了传感探头附近探针分子的拉曼散射信号,由此产生的背向拉曼散射光信号又通过光纤本身经由端面传输到光谱分析系统。为了减小随机误差,进行多次检测,并计算每个拉曼数据的平均值。

2.5　材料与仪器

样品表面的形态用扫描电子显微镜(SEM,Quattro S,赛默飞世尔公司)表征,拉曼测试实验在共聚焦拉曼光谱仪(LabRAM HR Evolution,Horiba Jobin Yvon S. A. S)上进行,激发波长为 532 nm,功率为 2.5 mW,积分时间为 10 s。使用 LapSpec 软件去除原始拉曼光谱的基线。

3　结果与讨论

3.1　SEM 和 EDS 表征

对制备的样品进行 SEM 分析,结果如图 2(a_1)、(a_2)所示,可观察到金属纳米粒子在光纤表面均匀分布,基本呈单层排列。此外,由于拉锥机制备的锥形光纤梯度小(锥尖角度为 5°~10°左右),较长的锥形区域可以更有效地富集金属粒子,有助于获得更低的检测极限。

为了更好地观察基底上 AgNPs 和 AuNPs 的富集情况,使用 energy dispersive spectrometer(EDS)对如图 2(b)的基底进行表征,结果如图 2(c)、(d_1)、(d_2)所示。可以清楚地看到,双金属锥形光纤 SERS 基底主要由 Si、O、Ag、Au(Ag:黄色;Au:粉红色)组成,Si、O 元素来自光纤,而 Ag 和 Au 元素则均匀地分布在光纤

的表面上，其质量分数分别为 2.36% 和 9.21%。对图 2(b)中的粒子进行粒径以及间隙的统计，结果如图 2(e_1)、(e_2)所示，可以看到，样品上金属粒子的平均粒径为 49 nm，平均间隙为 6.8 nm。

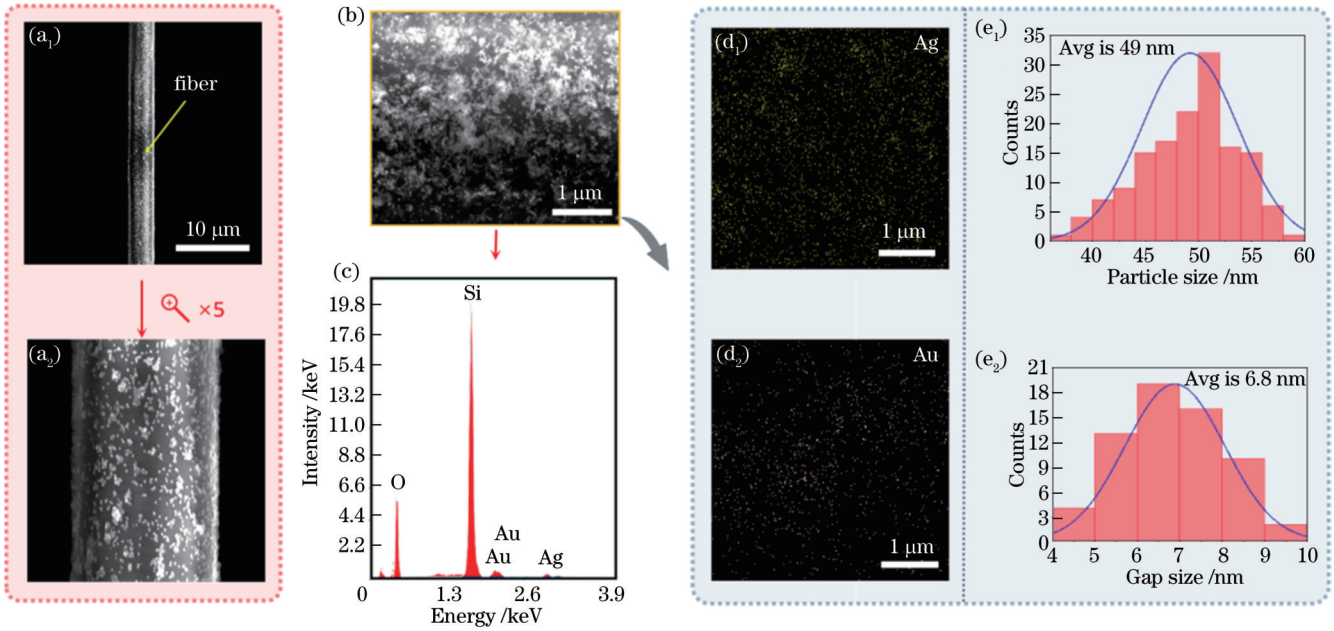

图 2　锥形光纤 SERS 探针表征图。(a_1)(a_2) SEM 图；(b) 进行 EDS 分析的 SEM 图；(c) 对锥形光纤 SERS 探针表面的元素类型进行 EDS 分析；(d_1)(d_2) 元素分布；(e_1) 粒径统计；(e_2) 间隙统计

Fig. 2　Characterization of the tapered optical fiber SERS probe. (a_1)(a_2) SEM images; (b) SEM image for EDS analysis; (c) EDS analysis of the element types on the surface of the tapered optical fiber SERS probe; (d_1)(d_2) element distribution; (e_1) statistical results of particle size; (e_2) statistical results of gap size

3.2　双金属富集机理

当锥形光纤尖端浸没在双金属纳米粒子混合溶液中时，激光通过光纤芯传播到锥形端，大部分功率从光纤尖端锥形区逃逸形成倏逝场，倏逝场与周围介质中的纳米粒子相互作用，产生散射力和梯度力。当梯度力远远大于散射力时，形成的合力便会将金属纳米粒子拉向锥形光纤表面[19-21]，如图 3(a_1)所示。

当锥形光纤从溶液拉至空气中后，由于上述力及表面张力的作用，锥形光纤表面存在携带大量金属纳米粒子的溶胶[15]。为了深入探究锥形光纤表面金属纳米粒子的自组装机理，利用 Comsol Multiphysics 多物理软件进行模拟分析。在波长为 632.8 nm、x 方向偏振的激光照射下，将直径为 49 nm 的金属纳米球置于水环境中的二氧化硅表面上，并选择第 1 部分进行分析，如图 3(a_2)所示。结果如图 3(b)、(c)所示，其中：图 3(b_1)、(b_2)、(b_3)分别为 AuNP 的温度场、三维流速场、二维流速场；图 3(c_1)、(c_2)、(c_3)分别为 AgNP 的温度场、三维流速场、二维流速场。仿真结果显示，胶体液滴中的金属纳米粒子能够有效吸收激光能量并将其转化为热量，从而使粒子周围的液体流速显著增加，提高蒸发速率。待粘附在纤维表面上的胶体液滴不均匀蒸发后，金属纳米粒子便会在光纤表面形成自组装[22]。此外，金纳米粒子在激光诱导下的温度场和流速场具有更大更广的梯度分布，更有利于其在光纤(二氧化硅)表面的吸附。

3.3　电磁场数值计算

为了探究双金属锥形光纤 SERS 的理论机理，使用 Comsol Multiphysics 计算二维光纤上的电磁场分布。根据之前金属纳米粒子尺寸和间隙的统计数据，设置金属粒子的直径为 49 nm，粒子间隙为 6.8 nm。根据 EDS 分析结果以及单个金、银纳米粒子的密度(金为 19.3 g/cm^3，银为 10.53 g/cm^3)，将光纤表面的金和银排列为规则的 Au-Au-Ag 结构(金和银粒子数比为 2∶1)。此外，设置入射激光波长为 532 nm，沿 x 轴偏振，并沿 z 轴传播，将周围介质设置为空气，并使用完美匹配层(PML)作为边界条件，如图 4(a)所示。其数值分析结果如图 4(b)所示，其中，锥形光纤尖端的电磁场分布如图 4(c)所示。光纤纤芯 A 点到原点 O_1 点的电场分布如图 4(d_1)所示。金属纳米粒子中心 B 点到 O_2 点的电场分布如图 4(d_2)所示。金属纳米粒子之间存在极强的电场强度，最大电场幅值为 16.8 V/m。

为了表征拉曼增强效果，采用理论的拉曼增强因子(F_{EF})来表征，其表达式为

$$F_{EF}=\frac{\left|E_{out}(\omega_0)\right|^2\left|E_{out}(\omega_s)\right|^2}{\left|E_0\right|^4}\approx\frac{\left|E_{out}\right|^4}{\left|E_0\right|^4},\tag{1}$$

式中：E_0 为入射电场强度大小，E_0=1 V/m；$E_{out}(\omega_0)$和 $E_{out}(\omega_s)$分别表示为入射光(频率 ω_0)和拉曼散射光(频

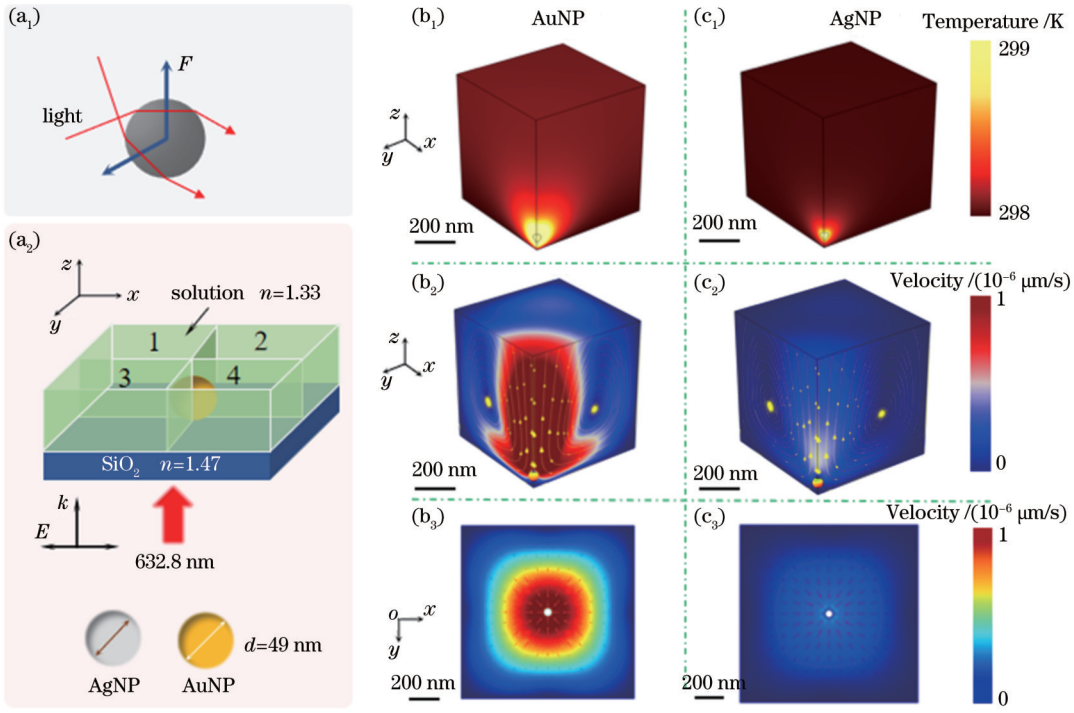

图 3　纳米粒子富集原理图。(a_1) 粒子受力示意图；(a_2) 模型示意图；(b_1) AuNP 温度场；(b_2) AuNP 三维流速场；(b_3) AuNP 二维流速场；(c_1) AgNP 温度场；(c_2) AgNP 三维流速场；(c_3) AgNP 二维流速场

Fig. 3　Schematic of silver nanoparticle enrichment. (a_1) Stress of nanoparticle; (a_2) schematic diagram of the simulation model; (b_1) temperature field of AuNP; (b_2) 3D velocity field of AuNP; (b_3) 2D velocity field of AuNP; (c_1) temperature field of AgNP; (c_2) 3D velocity field of AgNP; (c_3) 2D velocity field of AgNP

率为 ω_s) 的电场幅值。由于最大电场幅值为 16.8 V/m，根据式(1)，理论的最大 F_{EF} 约为 7.97×10^4。

进一步，为了研究金银纳米粒子的间隙、直径以及锥形光纤的锥尖角度对局域电场增强的影响，先对粒子间隙(固定锥形光纤角度为 5°，金属纳米粒子直径 49 nm，粒子间隙取 2、5、6.8、8、10 nm)进行扫描，再对金属纳米粒子直径(固定锥形光纤角度为 5°，金属纳米粒子间隙 6.8 nm，粒子直径取 20、30、49、60、80 nm)进行扫描，最后对锥形光纤角度(固定金属纳米粒子间隙 6.8 nm，粒子直径 49 nm，锥形光纤角度取 3°、4°、5°、8°、10°)进行扫描，得到的最大电场强度如图 5 所示。从图 5 可以清楚看到，在粒子间隙为 5 nm、粒径为 60 nm、角度为 4°时，各自有最大的电场强度。

3.4　拉曼实验

3.4.1　最低检测浓度

为了探究双金属光纤 SERS 探针的增强效应，采用 R6G 作为探针分子并利用上述测试方法进行拉曼测试，结果如图 6(a)所示。结果表明，该探针的最低检测浓度可达 10^{-10} mol/L。采用分析增强因子(F_{AEF})来描述实验的拉曼增强效应，其计算表达式为

$$F_{AEF}=\frac{I_{SERS}/c_{SERS}}{I_{RS}/c_{RS}},\tag{2}$$

式中：I_{SERS} 和 c_{SERS} 分别表示 SERS 条件下的拉曼信号和 R6G 浓度；I_{RS} 和 c_{RS} 分别表示非 SERS 条件下的拉曼信号和 R6G 浓度。其中，I_{SERS}=444.334，$c_{SERS}=10^{-10}$ mol/L，I_{RS}=215.076，$c_{RS}=10^{-2}$ mol/L。最终，样品的 F_{AEF} 为 2.07×10^8。与理论仿真结果相比，实验结果存在一定差异，主要原因有两点：首先，仿真结果只考虑了电磁场增强的贡献，未能考虑到化学增强效应；其次，仿真模型中金银纳米粒子是完全均匀分布的，以 6.8 nm 的间距排列，而在实际实验中，金属纳米结构可能存在少量聚集现象，粒子间距比设置的 6.8 nm 更小，因此会更加突显局域表面等离子共振特性。

3.4.2　多分子检测

为了验证样品对非单一分子的检测效果，使用 10^{-6} mol/L 的 R6G 和 10^{-4} mol/L 的 CV 混合溶液作为探针分子进行实验，结果如图 6(b)所示。测试结果表明，不同探针分子的独特拉曼峰(R6G：611 cm^{-1}、770 cm^{-1}、1650 cm^{-1} 等；CV：913 cm^{-1}、1188 cm^{-1}、1614 cm^{-1})在混合溶液中均能被检测到。

3.4.3　样品时效性测试

为了研究所提双金属光纤 SERS 探针的时效性(稳定性)，将制备的双金属光纤探针放置 24 h、48 h、72 h、96 h 后，对 10^{-7} mol/L R6G 的拉曼测试结果进行比较，结果如图 7(a)所示。

取 611 cm^{-1} 的拉曼强度，其变化趋势作如图 7(b)

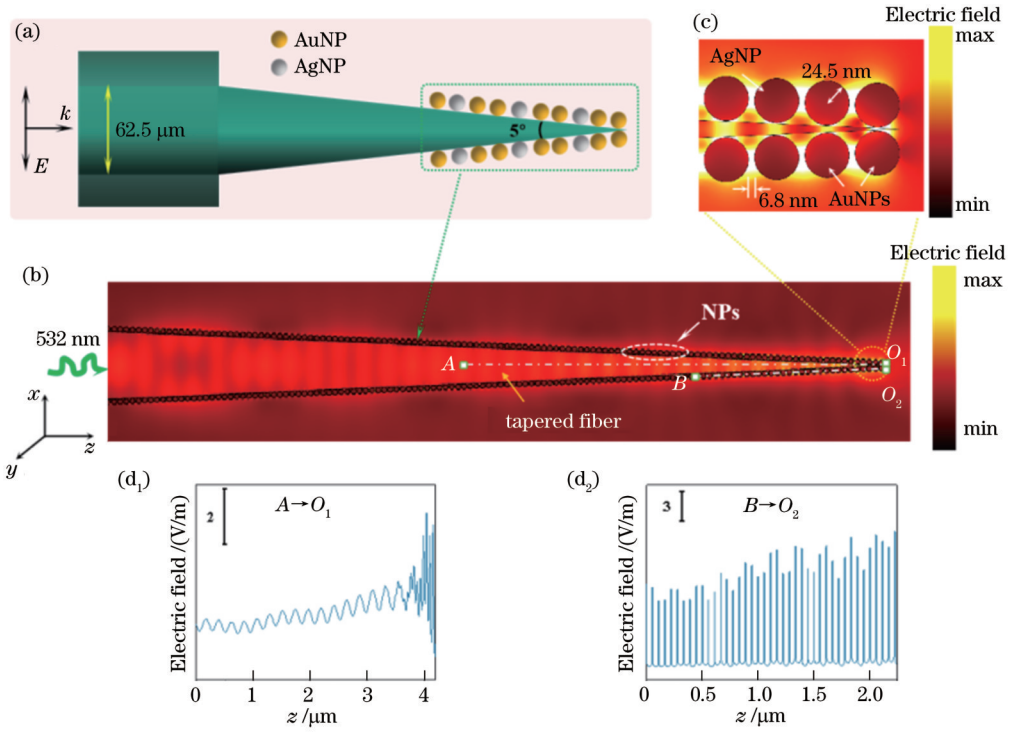

图 4　电磁场仿真图。(a) 锥形光纤 SERS 探针示意图；(b) 光纤前端电场强度仿真图；(c) 尖端部分放大的电场图；(d_1)(d_2) A-O_1和 B-O_2的电场强度

Fig. 4　Simulation of electromagnetic field. (a) Schematic diagram of the tapered optical fiber SERS probe; (b) simulation of electric field intensity at the front end of the fiber; (c) enlarged electric field map at the tip; (d_1) (d_2) electric field intensity from point A to O_1 and B to O_2

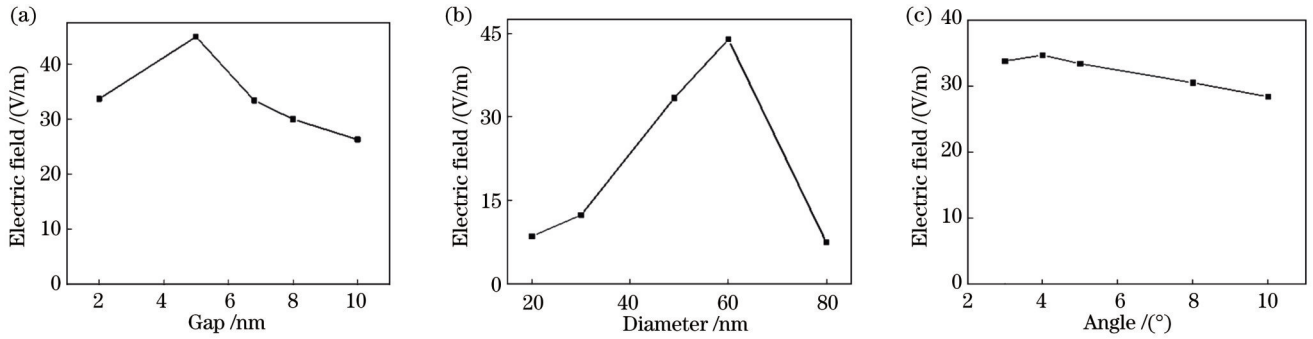

图 5　最大电场强度图。(a) 不同粒子间隙；(b) 不同粒子直径；(c) 不同锥形光纤角度

Fig. 5　The maximum electric field intensity maps. (a) Different gaps; (b) different diameters; (c) different angles

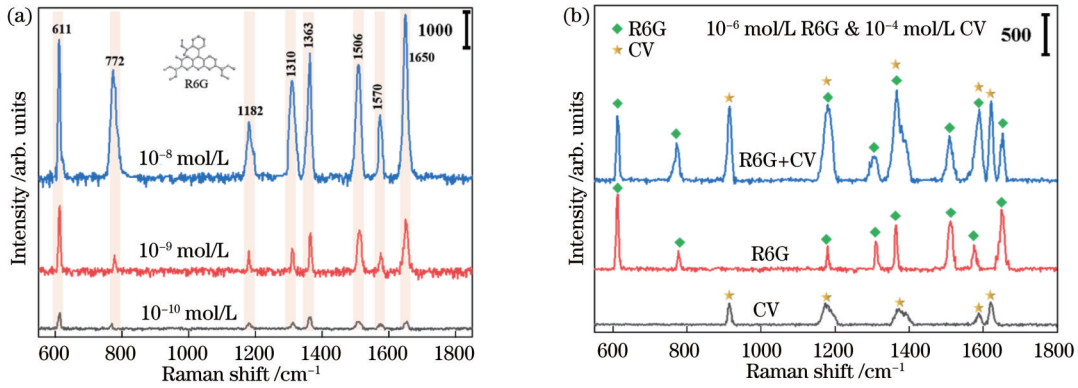

图 6　拉曼实验结果。(a) R6G 测试结果；(b) R6G 和 CV 混合物测试结果

Fig. 6　Raman measurements. (a) Test results of R6G ; (b) test results of R6G and CV mixture

所示。在放置 96 h 后，611 cm^{-1}的拉曼强度仍然有初始值的 16%，是单金属基底 2% 的 8 倍，这主要是因为银纳米粒子在空气中容易被氧化，而金纳米粒子的化学性更稳定些。

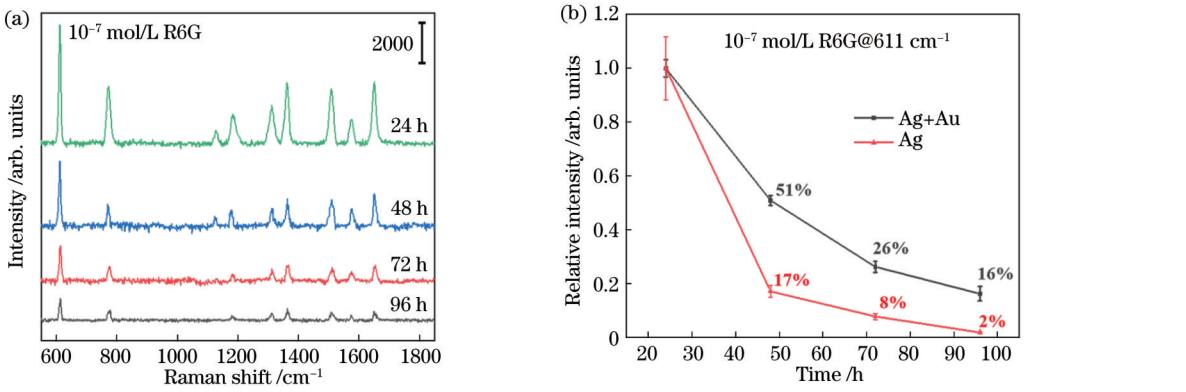

图 7 时效性实验。(a) 双金属光纤 SERS 探针的时效性测试结果；(b) 单金属和双金属光纤 SERS 探针 611 cm^{-1}的峰强随时间变化的比较

Fig. 7 Time-sensitive experiments. (a) Results of bimetallic SERS probes; (b) relative results of single Ag and bimetallic SERS probes at 611 cm^{-1} with R6G as analyte

4 结 论

提出一种新型双金属纳米粒子修饰锥形光纤 SERS 探针，实现了对低浓度 R6G 的检测和多分子的识别，该样品具有良好的 SERS 增强性能(F_{AEF}=2.07×10^8)和稳定性(96 h 后，双金属光纤 SERS 探针稳定性是单金属的 8 倍)。该双金属锥形光纤 SERS 探针未来有望在原位和远程检测方面得到应用。下一步研究方向是探索可控的双金属修饰光纤关键工艺，以进一步优化样品的检测灵敏度和稳定性。

参 考 文 献

[1] Müller Molnár C, Cintă Pînzaru S, Chis V, et al. SERS of cylindrospermopsin cyanotoxin: prospects for quantitative analysis in solution and in fish tissue[J]. Spectrochimica Acta Part A: Molecular and Biomolecular Spectroscopy, 2023, 286: 121984.

[2] Kanioura A, Geka G, Kochylas I, et al. SERS determination of oxidative stress markers in saliva using substrates with silver nanoparticle-decorated silicon nanowires[J]. Biosensors, 2023, 13(2): 273.

[3] Yang C P, Kao W Y, Yu S H, et al. Environmentally friendly etchant of *in situ* plasmon-activated water to improve SERS sensing of pesticides[J]. Sensors and Actuators B: Chemical, 2023, 374: 132798.

[4] Ge K, Huang Y H, Zhang H Q. Fabrication of hierarchical β-Bi_2O_3/AuAg microspheres for sensitive, selective and rapid detection of environment pollutants by surface-enhanced Raman spectroscopy[J]. Spectrochimica Acta Part A: Molecular and Biomolecular Spectroscopy, 2023, 285: 121907.

[5] Wang H Q, Liu M J, Zhao H M, et al. Rapid detection and identification of fungi in grain crops using colloidal Au nanoparticles based on surface-enhanced Raman scattering and multivariate statistical analysis[J]. World Journal of Microbiology and Biotechnology, 2023, 39(1): 26.

[6] Wang X J, Zhu X P, Tao Y F, et al. ZnO nanorods decorated with Ag nanoflowers as a recyclable SERS substrate for rapid detection of pesticide residue in multiple-scenes[J]. Spectrochimica Acta Part A: Molecular and Biomolecular Spectroscopy, 2023, 290: 122277.

[7] Fleischmann M, Hendra P J, McQuillan A J. Raman spectra of pyridine adsorbed at a silver electrode[J]. Chemical Physics Letters, 1974, 26(2): 163-166.

[8] Gao C B, Hu Y X, Wang M S, et al. Fully alloyed Ag/Au nanospheres: combining the plasmonic property of Ag with the stability of Au[J]. Journal of the American Chemical Society, 2014, 136(20): 7474-7479.

[9] Bian X Y, Zhang G Y, Liu B, et al. One-pot synthesis of Au/Ag alloy@SiO_2 core-shell nanoparticles and their metal-enhanced fluorescence and surface-enhanced Raman scattering spectroscopies[J]. Journal of Nanoparticle Research, 2022, 24(2): 20.

[10] Shinki, Sarkar S. $Au_{0.5}Ag_{0.5}$ alloy nanolayer deposited on pyramidal Si arrays as substrates for surface-enhanced Raman spectroscopy[J]. ACS Applied Nano Materials, 2020, 3(7): 7088-7095.

[11] Li H Y, Zhang J L, Jiang L L, et al. Chiral plasmonic Au-Ag core shell nanobipyramid for SERS enantiomeric discrimination of biologically relevant small molecules[J]. Analytica Chimica Acta, 2023, 1239: 340740.

[12] Li T, Yu Z N, Wang Z K, et al. Optimized tapered fiber decorated by Ag nanoparticles for Raman measurement with high sensitivity[J]. Sensors, 2021, 21(7): 2300.

[13] Chen Z Y, Dai Z M, Chen N, et al. Gold nanoparticles-modified tapered fiber nanoprobe for remote SERS detection[J]. IEEE Photonics Technology Letters, 2014, 26(8): 777-780.

[14] Yu Z N, Wang Z K, Zhang J E. Preparation optimization for a silver cavity coupled tapered fiber SERS probe with high sensitivity[J]. Optical Materials Express, 2022, 12(7): 2835-2843.

[15] Liu Y, Liu R M, Ai C W, et al. Stick-slip-motion-assisted interfacial self-assembly of noble metal nanoparticles on tapered optical fiber surface and its application in SERS detection[J]. Applied Surface Science, 2022, 602: 154298.

[16] Cao J, Zhao D, Mao Q H. A highly reproducible and sensitive fiber SERS probe fabricated by direct synthesis of closely packed AgNPs on the silanized fiber taper[J]. Analyst, 2017, 142(4): 596-602.

[17] Sha H Y, Wang Z K, Zhang J E. SiO_2 microsphere array coated by Ag nanoparticles as Raman enhancement sensor with high sensitivity and high stability[J]. Sensors, 2022, 22(12): 4595.

[18] 田茂杰，向小芳. 合成不同粒径大小的金纳米粒子的分析研究

[J]. 浙江化工, 2018, 49(3): 32-34.
Tian M J, Xiang X F. Analysis and study on the synthesis of gold nanoparticles with different particle sizes[J]. Zhejiang Chemical Industry, 2018, 49(3): 32-34.
[19] Kaur N, Trevisanutto J O, Das G. Tweezing and manipulating the distribution of gold nanorods (GNRs) on a tapered optical fiber to develop a plasmonic structure[J]. OSA Continuum, 2020, 3(9): 2415-2422.
[20] Trevisanutto J O, Linhananta A, Das G. Plasmonic structure: fiber grating formed by gold nanorods on a tapered fiber[J]. Optics Letters, 2016, 41(24): 5789-5792.
[21] Kaur N, Trevisanutto J O, Das G. Plasmonic structure on a tapered optical fiber for application as a surface-enhanced Raman spectroscopy substrate[J]. Microwave and Optical Technology Letters, 2021, 63(11): 2776-2781.
[22] Zhou F, Liu Y, Wang H C, et al. Au-nanorod-clusters patterned optical fiber SERS probes fabricated by laser-induced evaporation self-assembly method[J]. Optics Express, 2020, 28(5): 6648-6662.

Raman Enhancement Characteristics of Bimetallic Tapered Optical Fiber Surface-Enhanced Raman Scattering Probe

Huang Bo, Wang Zhengkun, Zhu Yong*, Zhang Jie

Key Laboratory of Optoelectronic Technology and System, Education Ministry of China, Chongqing University, Chongqing 400044, *China*

Abstract

Objective Surface-enhanced Raman scattering (SERS) is a powerful analytical tool that can provide molecular vibrational fingerprint information. Due to its unique analytical advantages, SERS has been widely applied in various fields such as biomedical research, environmental monitoring, and food analysis. During the development of SERS technology, silver nanoparticles have often been used as SERS substrates due to their excellent localized surface plasmon resonance properties. However, their susceptibility to oxidation poses a significant limitation in the construction of nano-probes for practical applications. In contrast, gold nanoparticles have better chemical stability and lower biotoxicity but relatively weaker Raman signal enhancement capability. Therefore, bimetallic SERS substrates combining gold and silver are characterized by high sensitivity and stability. Compared with traditional substrates, tapered optical fibers not only have the advantages of in-situ detection and remote signal transmission but also have great potential for enhancing laser reflection and improving light collection capability, which is beneficial for collecting weak Raman signals and achieving lower detection limits. Therefore, we proposed a simple and cost-effective bimetallic tapered optical fiber SERS probe. This probe utilized a light-induced method to deposit gold and silver nanoparticles on the surface of the tapered optical fiber, providing high sensitivity and good stability.

Methods The bimetallic tapered optical fiber SERS probe was prepared by using a light-induced method in this study. First, the tapered fiber was prepared by using the fiber fusion tapering machine. After clamping the processed fiber onto the fiber holder, the fiber fusion tapering machine was started to initiate the tapering process. Once the machine stopped operating, two tapered optical fibers were obtained. Second, gold and silver nanoparticles with an approximate diameter of 50 nm were prepared by using a chemical reduction method. Finally, the bimetallic tapered optical fiber SERS probe was prepared through the light-induced method. The laser beam emitted by a helium-neon laser was coupled into the tapered optical fiber. Subsequently, the tapered end was immersed in a mixed solution of Ag sol and Au sol (volume ratio of 1∶1, both 0.3 mL) for 60 seconds. Then, the tapered end was moved from the solution to the air and kept in that position for 90 seconds while the laser was still operating. This process was repeated 15 times [Fig. 1(a)]. At the end of the entire procedure, the bimetallic tapered optical fiber SERS probe was obtained. The surface morphology of the tapered optical fiber was characterized by scanning electron microscopy (SEM), and the performance of the optical fiber probe was tested by a confocal Raman spectrometer.

Results and Discussions In this study, SEM analysis [Fig. 2(a_1) and (a_2)] of the prepared samples revealed a uniform distribution of metal nanoparticles on the fiber surface, exhibiting a mostly monolayer arrangement. The relative mass percentages of Ag and Au elements were found to be 2.36% and 9.21%, respectively [Fig. 2(b) and (c)]. The average particle size of the metal particles on the sample was 49 nm, with an average gap of 6.8 nm [Fig. 2(e_1) and (e_2)]. In the paper, Rhodamine 6G (R6G) was selected as the analyte molecule to evaluate the SERS performance of the prepared samples. The bimetallic tapered optical fiber SERS probe was immersed in R6G solutions with concentrations ranging from 10^{-8} to 10^{-10} mol/L for three minutes respectively. After removal from the solution and natural drying, Raman signal

detection was performed, and the obtained enhancement factor (AEF) for the samples reached 2.07×10^{8}. To demonstrate the capability of detecting non-single molecule analytes, the samples were immersed in a mixed solution of 10^{-6} mol/L R6G and 10^{-4} mol/L crystal violet (CV) for three minutes. After removal from the solution and natural drying, the detection was conducted, and the results indicated that the unique Raman peaks of different probe molecules could be detected in the mixed solution [Fig. 6(b)]. To demonstrate the excellent stability of the bimetallic tapered optical fiber SERS probe, it was placed for different durations of 24 hours, 48 hours, 72 hours, and 96 hours. Afterward, a comparison was made by using Raman testing of 10^{-7} mol/L R6G. The results indicated that the sample exhibited good stability (Fig. 7).

Conclusions In this study, to enhance the enriched density of metal nanoparticles on the surface of optical fibers and improve the stability of the Raman-enhancing properties of the optical fiber SERS composite structure, we proposed a bimetallic (gold and silver) tapered optical fiber SERS probe structure. First, gold and silver nanoparticles with uniform morphology were prepared using the chemical reduction method. Then, the bimetallic particles were enriched on the tapered optical fiber using light-induced methods. The prepared optical fiber SERS probe exhibited excellent experimental performance. In this study, the lowest detected concentration of R6G was as low as 10^{-10} mol/L, and the enhancement factor was 2.07×10^{8}; compared with single-metal silver optical fiber SERS probes, the stability of the bimetallic sample was improved by seven times (after 96 hours). The bimetallic tapered optical fiber SERS probe is expected to be applied in in-situ and remote detection in the future. The next research direction is to explore the key process of controllable double metal modified optical fiber, so as to further optimize the detection sensitivity and stability of the sample.

Key words scattering; Raman scattering; bimetallic; tapered optical fiber; light-induced